ORIGINAL ARTICLE

Molecular Plant Pathology WILEY

Comparative transcriptional analysis of *Persea americana* *MYB*, *WRKY* and *AP2/ERF* transcription factors following *Phytophthora cinnamomi* infection

Alicia Fick[1,2] | Velushka Swart[1,2] | Aureliano Bombarely[3] | Noëlani van den Berg[1,2]

[1]Department of Biochemistry, Genetics and Microbiology, University of Pretoria, Pretoria, Gauteng, South Africa

[2]Hans Merensky Chair in Avocado Research, Forestry and Agricultural Biotechnology Institute, University of Pretoria, Pretoria, Gauteng, South Africa

[3]Instituto de Biología Molecular y Celular de Plantas, Consejo Superior de Investigaciones Científicas-Universitat Politècnica de València (IBMCP-CSIC-UPV), Valencia, Spain

Correspondence
Noëlani van den Berg, Department of Biochemistry, Genetics and Microbiology, University of Pretoria, Pretoria 0002, South Africa.
Email: noelani.vandenberg@up.ac.za

Abstract

Plant cells undergo extensive transcriptional reprogramming following pathogen infection, with these reprogramming patterns becoming more complex when pathogens, such as hemibiotrophs, exhibit different lifestyles. These transcriptional changes are often orchestrated by MYB, WRKY and AP2/ERF transcription factors (TFs), which modulate both growth and defence-related gene expression. Transcriptional analysis of defence-related genes in avocado (*Persea americana*) infected with *Phytophthora cinnamomi* indicated differential immune response activation when comparing a partially resistant and susceptible rootstock. This study identified 226 *MYB*, 82 *WRKY*, and 174 AP2/ERF TF-encoding genes in avocado, using a genome-wide approach. Phylogenetic analysis revealed substantial sequence conservation within TF groups underscoring their functional significance. RNA-sequencing analysis in a partially resistant and susceptible avocado rootstock infected with *P. cinnamomi* was indicative of an immune response switch occurring in either rootstock after 24 and 6h post-inoculation, respectively. Different clusters of co-expressed *TF* genes were observed at these times, suggesting the activation of necrotroph-related immune responses at varying intervals between the two rootstocks. This study aids our understanding of avocado immune response activation following *P. cinnamomi* infection, and the role of the TFs therein, elucidating the transcriptional reprogramming disparities between partially resistant and susceptible rootstocks.

KEYWORDS
avocado, defence-related genes, ERF, MYB, *Phytophthora*, transcription factor, WRKY

1 | INTRODUCTION

Transcription factors (TFs) play a significant role during the activation of plant immune responses following pathogen infection, regulating the expression of the receptor-encoding genes that recognize invading pathogens, thereby initiating a cascade of immune reactions (Moore et al., 2011). These receptor proteins include pathogen-associated molecular pattern (PAMP), recognition receptors (PRRs) and nucleotide-binding leucine-rich repeat (NLR) receptor proteins (Jones & Dangl, 2006; Matzinger, 2007; Monteiro & Nishimura, 2018). Enhanced levels of pathogen resistance are often associated with higher expression of *PRR* and *NLR* genes, as they enable the recognition of a greater number of pathogen-derived molecules, leading to a stronger activation of the immune response (Andam et al., 2020; Palaniyandi & Muthuswamy, 2017). Consequently, the TFs that regulate the expression of these receptors are indirectly linked to enhanced resistance against various pathogens. Moreover, TFs can indirectly influence the type of immune response activated during the infection of pathogens with different lifestyles. For example, certain TFs are responsible for the transcriptional regulation of defence-related genes (DRGs) that recognize biotrophic pathogens, while other TFs regulate the expression of DRGs involved with the recognition of necrotrophic pathogens (Cui et al., 2015). Biotrophic-related immune responses may lead to the hypersensitive response (HR) and thus, localized programmed cell death (PCD)—an undesirable immune response against necrotrophic pathogens (Lai & Mengiste, 2013; Yun et al., 2023). Hemibiotrophic-related immune responses are complex, with a switch in plant immune response-type and DRG expression patterns when the pathogen transitions to the necrotrophic phase (Backer et al., 2022; Bahari et al., 2018; Duan et al., 2023; Yang et al., 2013). The misregulation of DRGs, and indirectly TFs, during this transition leads to increased susceptibility (Liao et al., 2022). Thus, TFs modulate plant immune responses and dictate the outcome of these immune responses. Three major families of TFs, namely MYB, WRKY, and AP2/ERFs, have been identified as significant regulators of DRG expression (Chen et al., 2019; Ng et al., 2018). These TFs recognize *cis*-elements that are abundant in the promoter sequences of various DRGs, including those encoding PRR and NLR proteins (Ding et al., 2020; Mohr et al., 2010).

MYB, WRKY and AP2/ERF proteins are divided into different groups, based on protein structure. MYB TFs can be divided into four groups, depending on the structure of the TF's DNA-binding domain and number of imperfect repeats (R): 1R (R1/R2/R3-MYB), 2R (R2R3-MYB), 3R (R1R2R3-MYB) and 4R (R1R2R2R1/R2-MYB) (Cao et al., 2020). R2R3-MYBs are the largest and most studied group of MYB TFs, with more than 120 R2R3-MYB members found in *Arabidopsis thaliana*—although their involvement in plant defences is less studied despite MYB-binding sites being abundant in DRG promoter sequences (Dubos et al., 2010; Falak et al., 2021; Fick, Swart, et al., 2022). WRKY TFs contain the highly conserved WRKYGQK amino acid sequence and can be grouped into three groups (Group I, II and III) based on the number of these WRKY motifs, and the type of zinc finger motif (Eulgem et al., 2000). The second group (Group II) can further be divided into five subgroups, based on the primary amino acid sequence (Mahiwal et al., 2024; Zhang & Wang, 2005). Group I contains two WRKY motifs and is the largest group in most plant species, whereas groups II and III contain one WRKY motif (Rushton et al., 2010). Group III is recognizable for having a different zinc finger motif compared to the zinc finger motif found in group II. AP2/ERFs are plant-specific TFs, mostly studied for their contribution towards activating immune responses following abiotic stress (Nakano et al., 2006). This TF family can be divided into four groups, namely the AP2 (Apetala2), DREB (dehydration-responsive element binding), ERF (ethylene-responsive factor) and RAVs (related to abscisic intensive 3/viviparous 1) (Feng et al., 2020; Ma et al., 2024; Nakano et al., 2006). The structure of each TF group within MYB, WRKY and AP2/ERFs has been shown to correlate with TF function, or activation stimulus (Bakshi & Oelmüller, 2014; Hernández-Hernández et al., 2020; Xie et al., 2019). Thus, some groups play a more significant role during plant immune response activation and may contribute towards different immune response types.

MYB TFs are associated with activating HR, as seen in *Arabidopsis* for the AtMYB30 TF that shows increased expression levels following *Xanthomonas campestris* pv. *campestris* infection (Daniel et al., 1999). Another *Arabidopsis* MYB, AtMYB96, induces salicylic acid (SA) biosynthesis and increases resistance levels towards *Pseudomonas syringae* pv. *tomato* DC3000 (Seo & Park, 2010). Thus, MYBs are more often associated with activating immune responses towards biotrophic pathogens (Ambawat et al., 2013; Berrocal-Lobo et al., 2002; Mengiste et al., 2003). Expression analysis following pathogen infection has shown that WRKYs are associated with enhanced resistance towards both biotrophic and necrotrophic pathogens (Wani et al., 2021). Multiple WRKY TFs have been shown to mediate (through association with NLR proteins) and activate effector-triggered immunity (ETI) responses, leading to increased resistance towards biotrophic pathogens (Deslandes et al., 2002; Shen et al., 2007). Other WRKYs have instead been shown to enhance resistance levels towards necrotrophic pathogens, including *Botrytis cinerea* and *Alternaria brassicicola*, through the activation of camalexin synthesis (Seo & Choi, 2015; Zheng et al., 2006). Thus, different WRKYs activate and repress different immune response types, which is influenced by the invading pathogen's lifestyle. The ERF group is most often associated with activating DRG expression following pathogen infection, due to this group being one of the main downstream regulatory factors in the ethylene (ET) signalling pathway. ET synthesis is activated during necrotrophic-related immune responses, thus linking ERF TFs to necrotrophic-related defence responses (Huang et al., 2020; Lorenzo et al., 2003). However, some ERFs may also contribute towards biotrophic-related responses—for example, the Pti4 and Pti5 ERFs are phosphorylated following *P. syringae* infection of tomato (*Solanum lycopersicum*), and contribute to enhanced resistance (Zhou et al., 1997). Each of these major TF families has also been implicated in the deposition of callose—a defence strategy aimed at restricting pathogen growth (Ali et al., 2013; Ellinger & Voigt, 2014; Pillai et al., 2018). Taken together, TF families play specific and complex roles in activating plant immune responses following pathogen infection.

As these TFs regulate growth, development and immune responses in plants, expression analysis of MYB, WRKY and AP2/ERFs during pathogen infection provides an opportunity to decipher which TFs are responsible for DRG regulation. Moreover, expression analysis following infection of a hemibiotroph would facilitate the identification of TF members that regulate DRG expression during both biotrophic and/or necrotrophic infection stages. Thus, this study used an RNA-seq approach to investigate the expression of MYB, WRKY and AP2/ERFs in two avocado (*Persea americana*) rootstocks infected with *Phytophthora cinnamomi*, a hemibiotrophic oomycete (Hardham & Blackman, 2018). This study is the first genome-wide identification of avocado *MYB* and *WRKY* genes. In a previous study, 134 AP2/ERF-encoding genes were identified using the *P. americana* 'Hass' genome, with 10 AP2/ERFs being implicated in fatty acid accumulation (Ge et al., 2021). However, the expression for all three TF families has never been studied during *P. cinnamomi* infection. We hypothesized that RNA-seq analysis of avocado *MYB*, *WRKY* and *AP2/ERFs* following *P. cinnamomi* infection would allow for the identification of the TFs that regulate DRGs. Furthermore, we hypothesized that different TF members would be expressed before and after 24 h post-inoculation (hpi), as previous studies indicated that *P. cinnamomi* transitions to a necrotrophic lifestyle between 18 and 24 hpi in a partially resistant rootstock (Dusa) (Backer et al., 2015; van den Berg et al., 2018, 2021). Thus, this analysis may serve as an indication of which TFs regulate biotrophic- or necrotrophic-related immune responses. *P. cinnamomi*, where present, poses the greatest threat to the avocado industry due to the difficulty of implementing control measures. As the avocado industry mainly relies on partially resistant rootstocks as a control method, understanding the molecular mechanisms behind successful immune responses against this pathogen can accelerate the identification of rootstocks with enhanced resistance levels.

2 | RESULTS

2.1 | *MYB* gene and protein analysis

In total, 226 putative MYB-encoding genes were identified from the genome following the removal of redundant sequences. Three repeat regions were identified using conserved motifs: motif 3 and 4 formed Repeat 1 (W-X_{40}-SHLQ), motifs (in specific order) 3, 6, 2 and 5 formed Repeat 2 (W-X_{18}-W-X_{18}-W), and Repeat 3 (F-X_{16}-W-X_{18}-W) consisted of motif 1 only (Figure 1). These repeats were used to categorize 162 sequences as being R2R3-MYB group members and 41 as being 1R-MYB group members. Of these 41 sequences, 33 sequences contained Repeat 1, four Repeat 2 and 10 Repeat 3 motifs only. No sequences were classified as 3R-MYB- or 4R-MYB-encoding TFs. Gene structure analysis showed that eight (3%) *MYB* genes were intronless, with five belonging to the R2R3-MYB group, and three being Repeat 1 1R-MYBs. Two of the 1R-MYB intronless genes were found to be paralogues, having high sequence similarity and being neighbouring genes on chromosome 1. Of the remaining

1R-MYBs, most (16) genes contained six exons with five introns. A large number of *MYB* genes (39%), most classified as R2R3-MYBs, contained three exons and two introns. Peame105C03g049450, a R2R3-MYB-encoding *MYB*, was found to have the highest number of exons (35) and introns (34). Phylogenetic relationships were analysed between avocado MYB and experimentally validated *Arabidopsis* MYB protein sequences, as this may provide some evidence regarding the functional significance of the PaMYBs (Figure S1). The results showed that most clades contained AtMYBs with either growth- or defence-related function. Thus, PaMYB proteins with similar sequences may be functionally related. However, six clades contained AtMYBs shown to have function in both growth and defence. Fifty PaMYB sequences, most 1R-MYBs, formed part of a large clade that did not contain any AtMYB sequences. Twenty-three sequences were uncategorized based on having incomplete repeat regions; however, InterPro analysis showed that these proteins still contained MYB binding sites. Furthermore, evolutionary relationships showed these genes contained motifs similar to complete MYB sequences within the same clade.

2.2 | *WRKY* gene and protein analysis

A total of 82 WRKY-encoding sequences were identified from the West-Indian pure accession genome. All these sequences contained at least one WRKY motif (WRKYGQK), followed by a C_2H_2-type zinc finger motif (C-X_4-C-X_{24}-H-X-H). MEME analysis identified two WRKY-containing motifs (motifs 1 and 3), with motif 1, together with motif 2 forming the zinc finger motif. The WRKY sequences were grouped into three major groups, based on the number of WRKY motifs and the motif identified upstream from the WRKY motif in each sequence (Figure 2). Group I included 13 WRKY sequences and contained two WRKY motifs and a downstream C_2H_2-type zinc finger motif. Group II, divided into five subgroups, contained the most PaWRKY sequences, with subgroup IIc being the largest of the subgroups containing 15 complete sequences. Subgroup IId was the second largest with 13 sequences, followed by subgroup IIe with 10 sequences. Subgroups IIa and IIb were the two smallest subgroups, with six and eight sequences, respectively. Lastly, 10 sequences were identified as group III sequences, with C-X_{24}-H-T zinc finger motifs. Phylogenetic analysis grouped all genes within the different groups and subgroups together, except for one IIe WRKY (Peame105C07g037370.1). This gene did not contain motif 5 or 11, which was present in other IIe WRKY sequences. Exon–intron boundaries showed that a large number (42%) of *WRKY* genes contained three exon and two introns; however, gene structure was not conserved between subgroup members. *WRKY* genes encoding I, IIa and IIb type proteins, mainly contained four to six exons and grouped closely together phylogenetically. Phylogenetic analysis performed to show the relationship between experimentally validated *Arabidopsis* WRKYs and PaWRKY sequences indicated that different PaWRKY groups were more closely related to AtWRKYs with immune response activation roles (Figure S2). WRKYs part of the IIe subgroup formed a clade with seven AtWRKYs shown to participate in plant
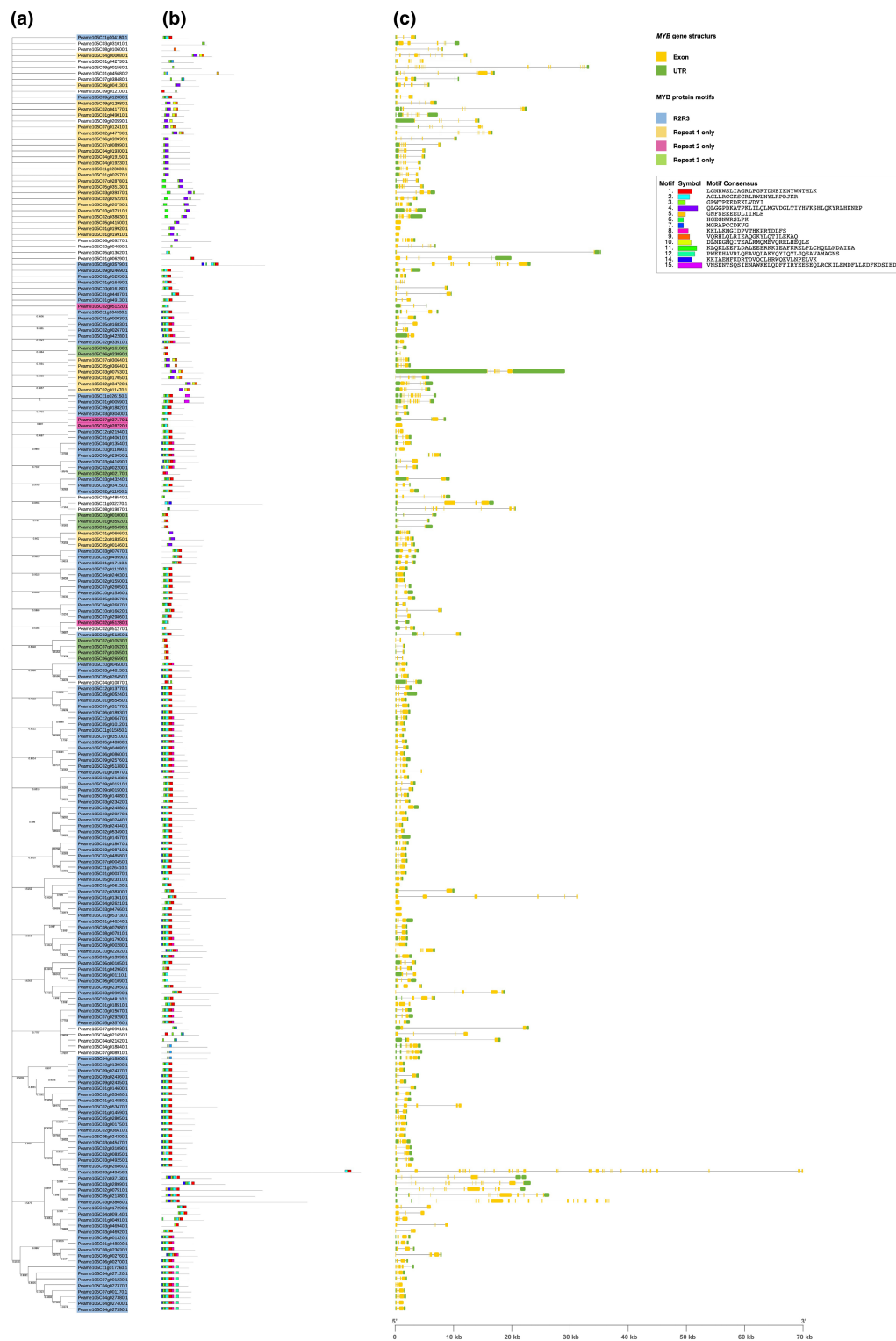
FIGURE 1 Gene and protein structures of 226 MYB sequences from the *Persea americana* 'West-Indian' pure accession genome. (a) Phylogenetic analysis was done using the neighbour-joining method, Jones–Thornton–Taylor (JTT) method and 1000 bootstrap following ClustalW alignment of PaMYB sequences. (b) Conserved motifs identified within MYB protein sequences using the MEME Suite online tool, with sequences corresponding to the indicated blocks being listed on the right of the figure. The conserved sequences were used to divide the sequences into different MYB subfamilies. (c) Exon–intron boundaries of the *MYB* genes, with gene sizes indicated in kilobase pairs (kb). Exons are represented by yellow boxes, introns by black lines and untranslated regions (UTRs) by green boxes (R2R3—R2R3-MYB; R1, R2 and R3—1R-MYB).
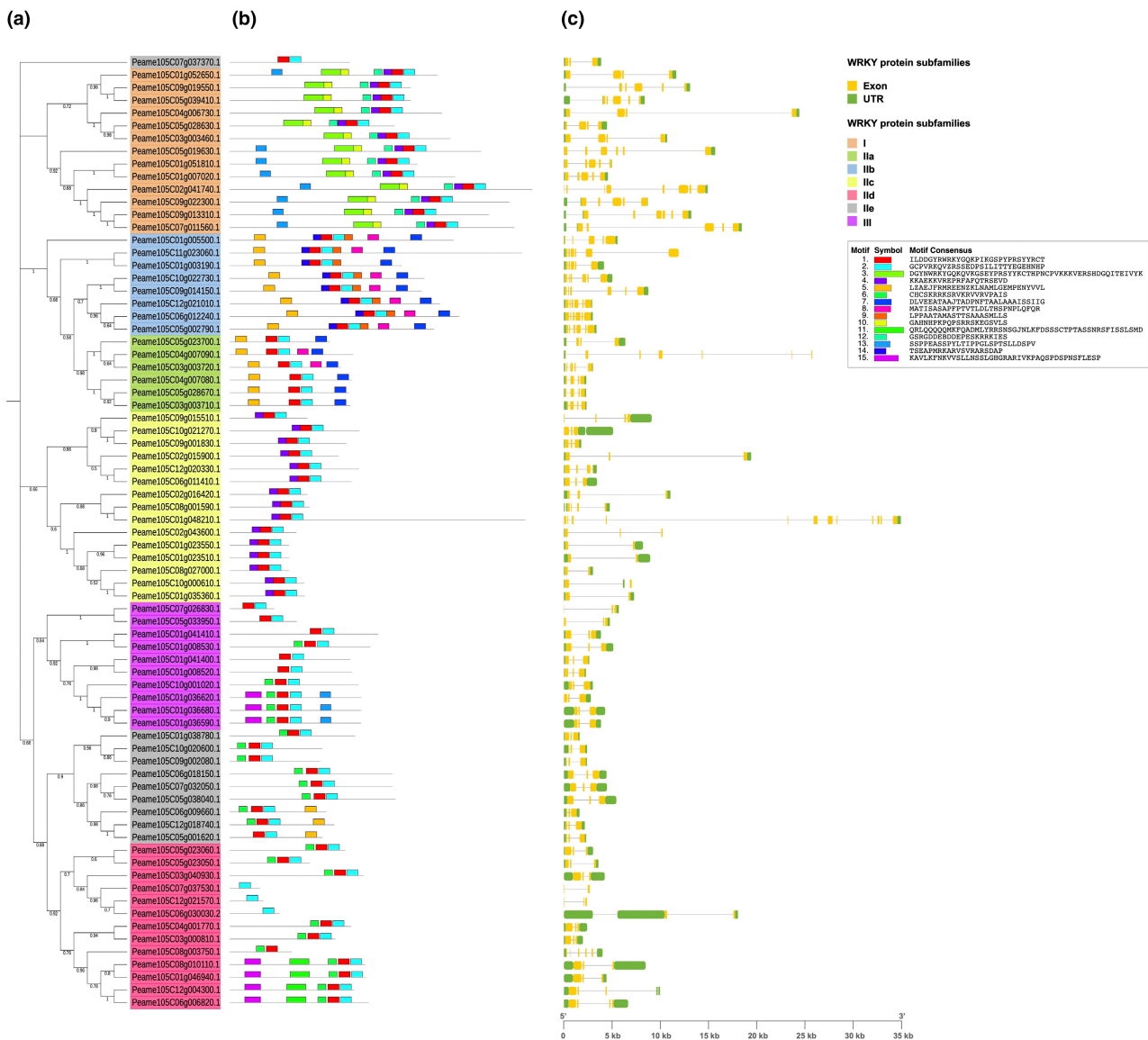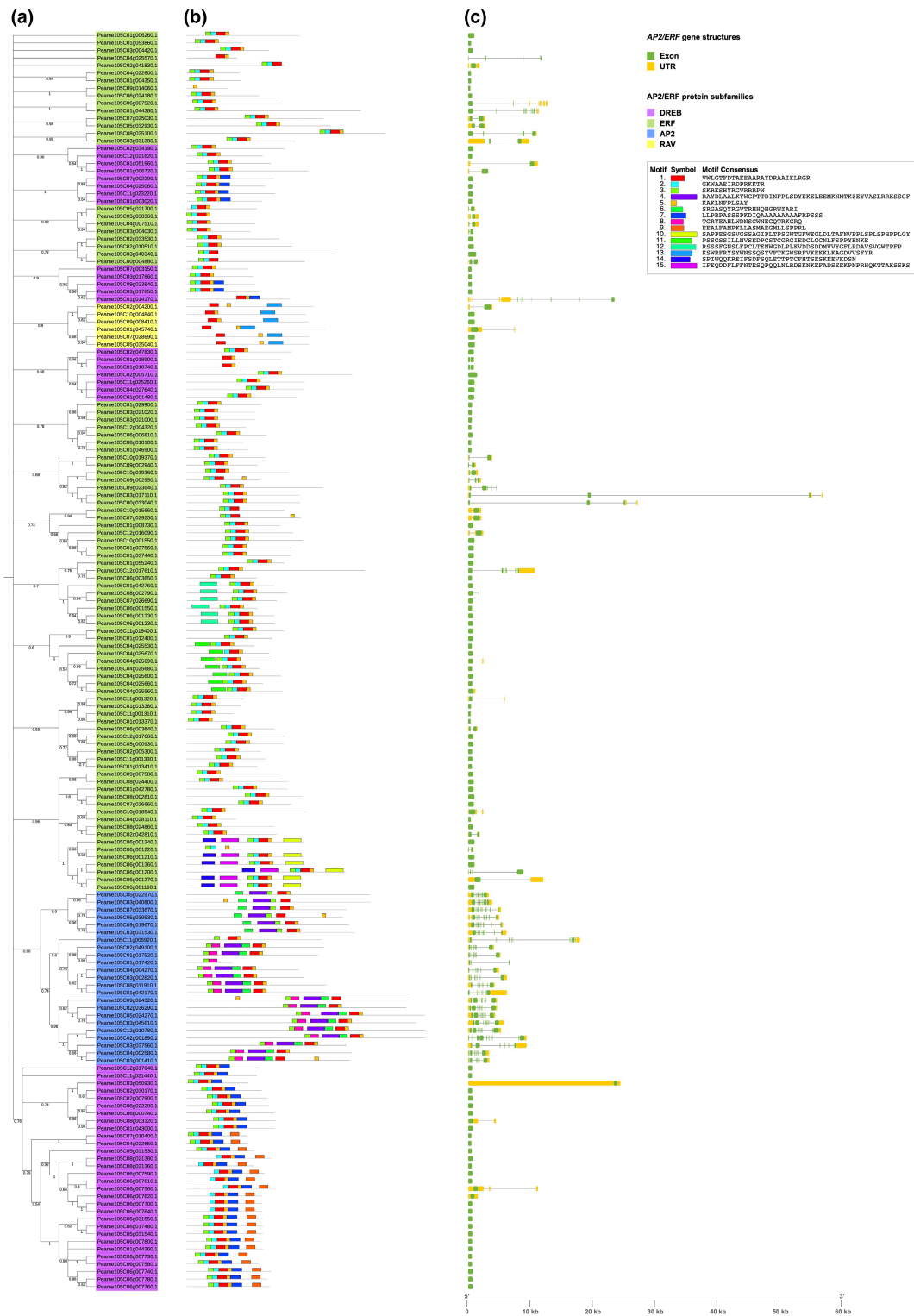
FIGURE 2 Conserved WRKY motifs and gene exon–intron boundaries from the *Persea americana* 'West-Indian' pure accession genome. (a) A neighbour-joining tree constructed using the Jones–Thornton–Taylor (JTT) method, with 1000 bootstrap replications, following ClustalW alignment of PaWRKY sequences. (b) The MEME online tool was used to identify 15 conserved motifs (sequences shown on the right of the figure) within 82 WRKY protein sequences. These motifs were used to assign WRKY proteins into different groups and subgroups, which are shown on the right in the phylogenetic tree. (c) WRKY gene exon–intron regions, with gene sizes indicated in kilobase pairs (kb). Yellow boxes indicate exons, green boxes indicate untranslated regions and black lines indicate introns.

immune responses (Bakshi & Oelmüller, 2014). Other subgroup members formed clades that grouped together with at least one AtWRKY shown to regulate cell development and growth (Rushton et al., 2010). One clade, formed with group I members in particular, was closely related to three growth-related AtWRKYs, while other clades only contained one growth-related AtWRKY sequence.

2.3 | *AP2/ERF* gene and protein analysis

In total, 174 *AP2/ERF* genes were identified in the West-Indian pure accession genome. Analysis of the conserved protein sequences categorized 50 proteins as members of the DREB protein group and

95 as ERF protein group members (Figure 3). In this study, 23 sequences were assigned as AP2 proteins, with 21 of these sequences containing two AP2 domains. Six sequences contained one AP2 motif followed by a B3 domain and were assigned as RAV proteins. Phylogenetic analysis grouped all AP2- and RAV-type sequences together; however, DREB and ERF sequences grouped into four and three main clades, respectively. Further protein analysis showed that one DREB (Peame105C04g027640) and two ERF proteins (Peame105C11g001310 and Peame105C01g013370) contain the activation EDLL motif (Tiwari et al., 2012). However, 24 sequences contained the repression EAR motif—eight with the DLNXXP consensus sequence, 14 with the LXLXL consensus sequence and two with the RLFGV (B3 repression domain) consensus sequence. All B3

FIGURE 3 Conserved motifs of AP2/ERF family proteins from the *Persea americana* 'West-Indian' pure accession genome, together with gene exon–intron boundaries. (a) A neighbour-joining phylogenetic tree constructed using the Jones–Thornton–Taylor (JTT) method, with 1000 bootstrap replications, following ClustalW alignment of PaAP2/ERF sequences. (b) Fifteen motifs within 174 sequences were identified using the MEME online tool, with the motif sequences being listed on the right of the figure. (c) Exon–intron boundaries of AP2/ERF-encoding genes, with gene sizes indicated with kilobase pairs (kb). Green boxes represent exons, yellow boxes represent untranslated regions and black lines represent intron regions.

repression domain-containing proteins belonged to the RAV group. Gene structure analysis showed that the number of introns varied among the different TF groups. All AP2-encoding genes contained between 4 and 10 introns, with 5–11 exons. Most (117; 67%) DREB-, ERF- and RAV-encoding gene sequences did not contain any introns. These intronless genes had no differences in conserved protein sequences when compared to genes with introns. Phylogenetic analysis with *Arabidopsis* AP2/ERF and Hass avocado AP2/ERF sequences showed that PaAP2/ERFs, part of the ERF group, were closely related to AtAP2/ERFs known to play a role during abiotic or biotic stress responses (Figure S3). PaAP2/ERFs that belong to the DREB and AP2 groups were more closely related to AtAP2/ERFs, which regulate cellular growth and differentiation. Furthermore, no PaAP2/ERF sequences grouped closely with the Hass Soloist sequence.

2.4 | Avocado *MYB* expression following *P. cinnamomi* infection

Of the 226 *MYB* TFs, 124 showed differential expression ($\log_2$FC ≥|1|, $p ≤ 0.05$) following *P. cinnamomi* inoculation at no less than one time point in either rootstock, when compared to mock-inoculated samples (Figure 4a). Of these *MYBs*, 90 encoded R2R3-MYBs, 18 R1-MYBs, 15 R3-MYBs and three R2-MYBs. Eight encoded MYBs belonging to an unknown subfamily. Most *MYB* genes, 53 in total, were upregulated (red-coloured block) at all time points in both the partially resistant Dusa and susceptible R0.12 rootstocks. Other *MYBs* were downregulated (blue-coloured block), with 33 *MYBs* being significantly downregulated in both rootstocks at 6 hpi. Very few significant changes in expression were observed in R0.12 at 12 and 24 hpi. Unexpectedly, genes with high protein sequence similarity to growth-related AtMYBs were upregulated at 6, 12 and 24 hpi in Dusa and at 6 hpi only in R0.12. Seven *PaMYBs* in particular had very high $\log_2$FC values during 6–24 hpi, and were all closely related to growth-related AtMYBs. Noticeably, a group of *PaMYB* genes that showed significantly higher expression levels at 120 hpi in both rootstocks had high sequence similarity to defence-related AtMYBs (Hernández-Hernández et al., 2020). Expression comparisons with R0.12 set as the reference (Figure 4b) showed very few differences in the level of *MYB* expression between the two rootstocks at 6 hpi and in the mock-inoculated samples (MI). The largest differences in expression were observed at 12 and 24 hpi, where most *MYB* genes had higher levels of expression in Dusa (red-coloured block). A large majority of these *PaMYB* genes were closely related to growth-related AtMYBs (Hernández-Hernández et al., 2020). Very few *PaMYB* genes closely related to defence-related AtMYBs showed expression level differences between the two rootstocks.
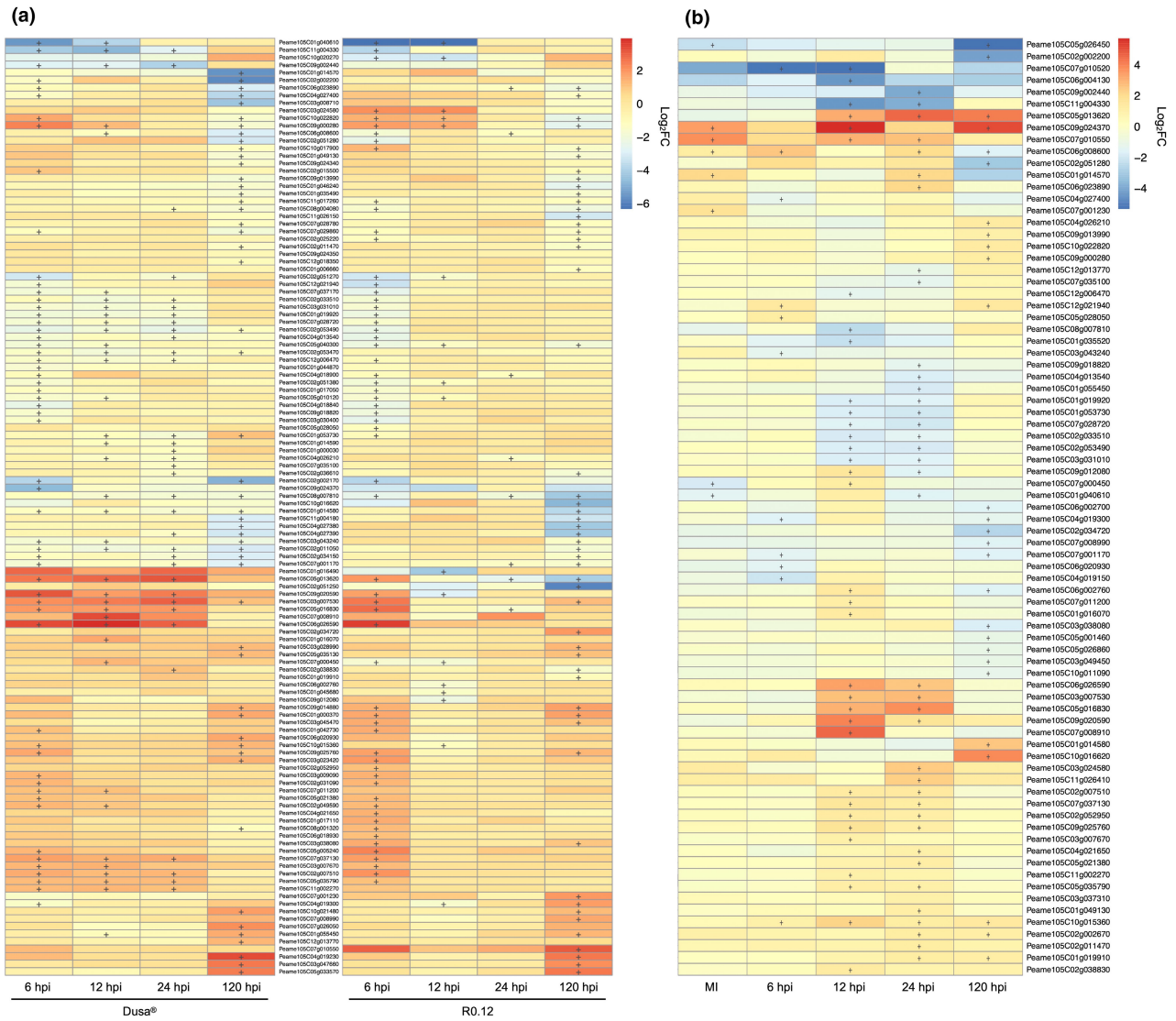
2.5 | Avocado *WRKY* expression following *P. cinnamomi* infection

Of the 82 *WRKY* genes, 50 showed significant differences in expression levels following *P. cinnamomi* inoculation when compared to mock-inoculated samples (Figure 5a). These included 12 IIe WRKYs, 10 IIc and III WRKYs, six I WRKYs, five IIb WRKYs, four IIa WRKYs and three IId WRKYs. Most expression level differences were observed at 120 hpi, where 25 *WRKYs* were upregulated (red block) in Dusa and 20 in R0.12. The majority of these *PaWRKY* sequences were closely related to defence-related AtWRKY sequences. At the earlier time points, one *WRKY* in particular (Peame105C09g019550) had the highest $\log_2$FC values at 6, 12 and 24 hpi in Dusa, but only at 6 hpi in R0.12. This gene has high sequence similarity to a growth-related AtWRKY sequence (Bakshi & Oelmüller, 2014). With R0.12 expression levels set as the reference, this gene also showed significantly higher expression levels (red block) in Dusa at 12 and 24 hpi (Figure 5b). This analysis also indicated that the largest and most significant differences in expression levels, when compared between the two rootstocks, occurred at 12 and 24 hpi. At these time points, 14 *WRKY* genes were expressed at higher levels in susceptible R0.12 (blue block). These *PaWRKYs* were generally closely related to defence-related AtWRKYs, while *PaWRKY* genes expressed at higher levels in Dusa were more closely related to growth-related AtWRKYs (Bakshi & Oelmüller, 2014; Rushton et al., 2010).

2.6 | Avocado *AP2/ERF* expression following *P. cinnamomi* infection

In total, the level of expression of 116 *AP2/ERFs* changed significantly in avocado rootstocks following *P. cinnamomi* inoculation compared to mock-inoculated samples (Figure 6a). Of these sequences, 64 encode ERF-type proteins, 35 encode DREBs, 12 encode AP2s and three encode RAVs. Most *AP2/ERF* genes had lower levels of expression (blue blocks) at 6 hpi in R0.12, and at 6, 12 and 24 hpi in Dusa. Two notable *AP2/ERFs*, Peame105C06g007640 and Peame105C02g034190, were expressed at much higher levels (red blocks) in Dusa following *P. cinnamomi* inoculation at 6, 12 and 24 hpi; however, a significant difference in expression level was only observed at 6 hpi for Peame105C02g034190 in R0.12. Both of these *PaAP2/ERFs* encoded DREB-type proteins and grouped closely with growth-related AtAP2/ERFs. AP2-encoding genes were never upregulated in Dusa at 6, 12 and 24 hpi; however, three AP2-encoding genes were upregulated at different time points in R0.12 (Peame105C02g012400 and Peame105C07g033670 at 6 hpi, and Peame105C06g007580 at 6 and 12 hpi). At 120 hpi, more AP2/ERF-encoding genes were upregulated significantly (red blocks), and with higher $\log_2$FC values, in Dusa (34 *AP2/ERFs*) compared to R0.12 (24 *AP2/ERFs*). The same was seen for AP2/ERFs-encoding genes, which were downregulated at 120 hpi, with more *AP2/ERF* genes being downregulated in Dusa (23 *AP2/ERFs*) compared to R0.12 (22 *AP2/ERFs*). Expression level comparisons with R0.12 set as the reference also confirmed that the level of *AP2/ERF* expression was significantly higher in Dusa (red blocks) at 120 hpi (Figure 6b). At 12 and 24 hpi, however, most *AP2/ERFs* showed higher levels of expression in R0.12 (blue blocks) compared to Dusa. Very few significant differences were observed between the two rootstocks in mock-inoculated samples and at 6 hpi.

FIGURE 4 *MYB* transcription factor expression patterns in partially resistant Dusa and susceptible R0.12 avocado rootstocks following *Phytophthora cinnamomi* inoculation. (a) Heatmap showing the $\log_2$fold-change ($\log_2$FC) in the expression of 118 *MYBs* in infected Dusa and R0.12 rootstocks, with mock-inoculated samples set as the reference. Cells with cross symbols indicate a significant difference in expression levels ($\log_2$FC ≥ |1|, $p ≤ 0.05$). A positive $\log_2$FC (red) indicates higher expression levels compared to that in mock-inoculated samples, and a negative $\log_2$FC (blue) indicates lower expression levels. (b) Heatmap showing the difference in the expression level (as $\log_2$FC) of 73 *MYBs* when Dusa samples are compared with R0.12 samples set as reference following *P. cinnamomi* inoculation. A positive $\log_2$FC (red) value indicates the level of expression is higher in Dusa compared to R0.12, and a negative $\log_2$FC (blue) value indicates higher expression levels in R0.12. Cross symbols indicate significant $\log_2$FC values (MI, mock-inoculated).

3 | DISCUSSION

MYB, WRKY and AP2/ERF TFs play significant roles during the activation of plant immune responses, due to different members within these TF families regulating expression levels of growth or DRGs. Members within these TF families may contribute to enhanced resistance towards biotrophic or necrotrophic pathogens by activating the relevant signalling pathways. Thus, studying the expression of the *MYB*, *WRKY* and *AP2/ERF* genes in avocado in response to *P. cinnamomi* provides a deeper understanding of avocado immune response activation. This is the first genome-wide study to identify *PaMYB* and *PaWRKY* genes and investigate the expression of *MYB*,

WRKY and *AP2/ERF* genes in avocado in response to a hemibiotrophic pathogen.

We identified 226 *PaMYB* and 82 *PaWRKY* genes in the West-Indian pure accession avocado genome. The total number of *TF* genes has previously been associated with genome size (Zhang et al., 2018, 2023); however, only 121 *CcMYBs* were identified in *Cinnamomum camphora*, a close relative to avocado and part of the *Lauraceae* family (Luan et al., 2022). These species have very similar genome sizes (*C. camphora*: 823 Mb; *P. americana*: 857 Mb), and it would be interesting to investigate possible *MYB* duplications in avocado (Chaw et al., 2019). Genome-wide identification of *Cinnamomum kanehirae WRKY* genes revealed 73 *CkWRKY*
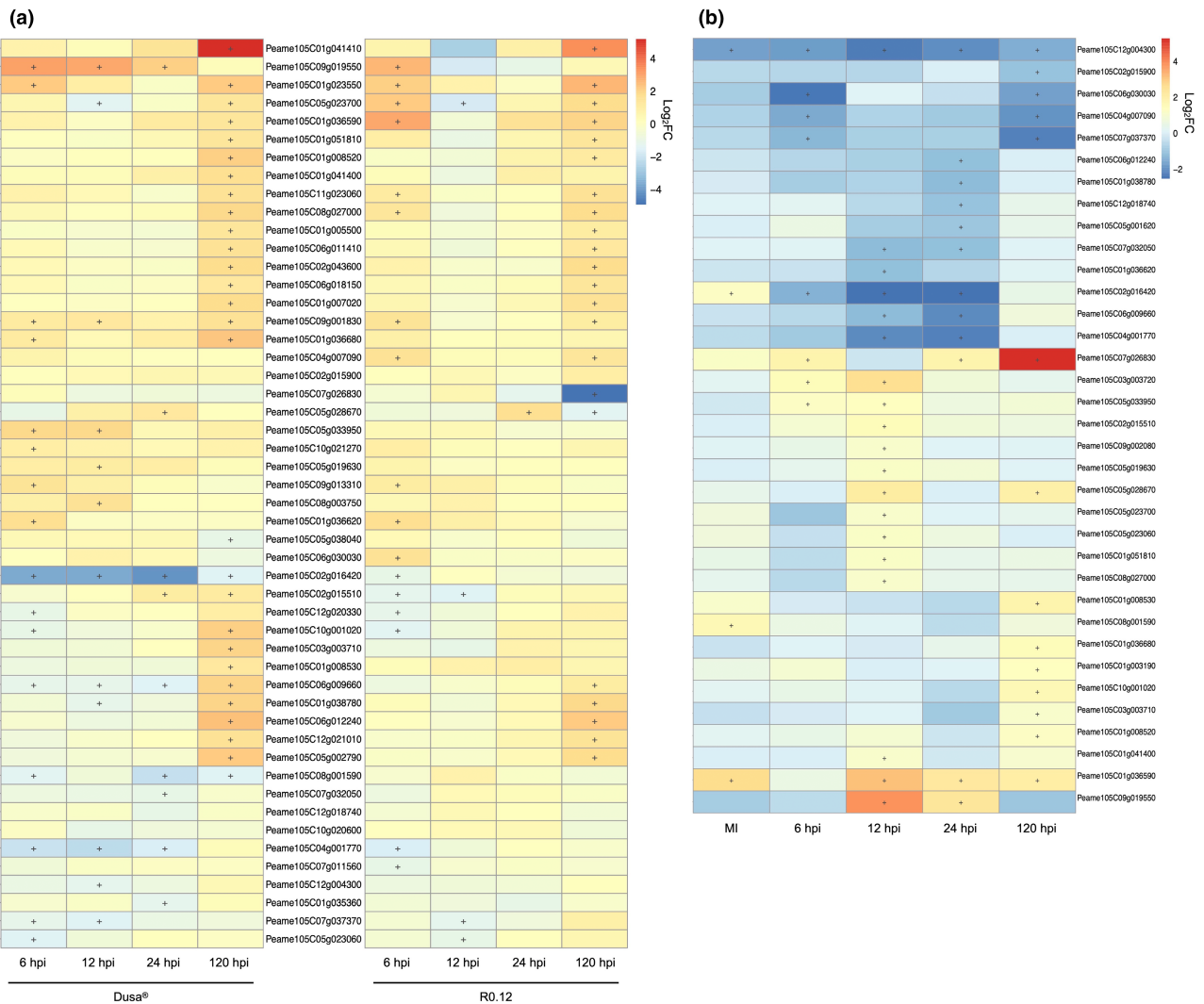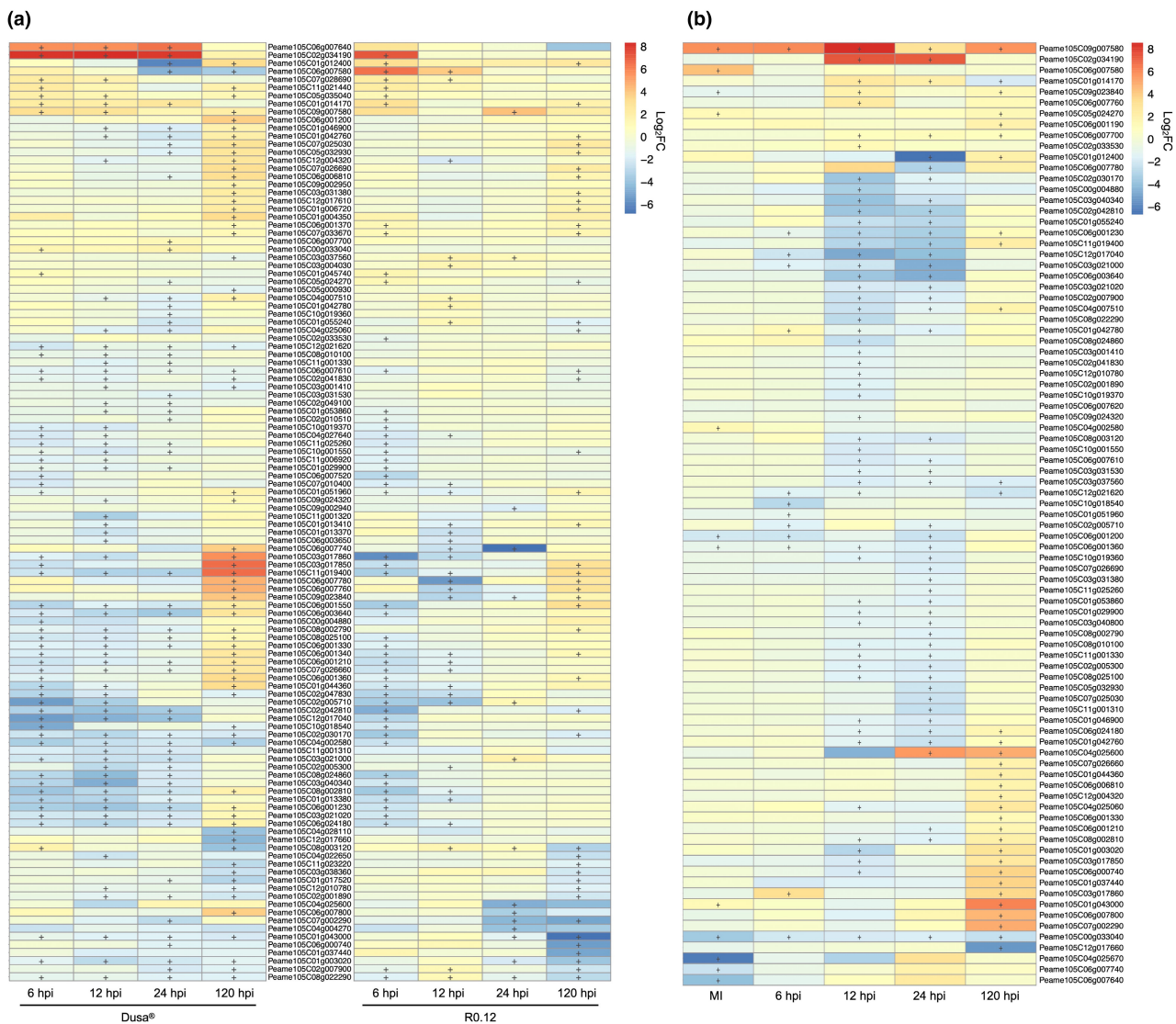
FIGURE 5 Expression level differences of *WRKY* genes in two avocado rootstocks following *Phytophthora cinnamomi* inoculation. (a) Heatmap of the differences in expression levels as $\log_2$fold-change ($\log_2$FC) in Dusa (partially resistant) and R0.12 (susceptible) rootstocks at different time points (hours post-inoculation; hpi) following inoculation. Mock-inoculated samples are set as the reference, thus positive $\log_2$FC values (red) indicate higher expression levels in inoculated samples, and negative $\log_2$FC values (blue) indicate lower expression levels in inoculated samples. (b) Heatmap showing the level of *WRKY* expression compared between the two rootstocks, with R0.12 set as the reference. Positive $\log_2$FC values (red) indicate higher *WRKY* expression levels in Dusa and negative $\log_2$FC values (blue) indicate higher levels of expression in R0.12. (+ symbols indicate significance, $\log_2$FC ≥ |1|, $p ≤ 0.05$; MI, mock-inoculated).

genes, comparable to the number in avocado (Chaw et al., 2019). Previously, 134 *AP2/ERF* genes were identified in the Hass avocado cultivar genome (Ge et al., 2021); however, this study identified 174 *AP2/ERF* genes. The West-Indian pure accession genome, used in this study, is of high quality and our study provides a more complete representation of avocado *AP2/ERF* genes. However, more RAV-type TFs were identified in the Hass genome, including a Soloist that was not identified in this study. This shows that there is variation in the number of *TF* genes within avocado germplasm.

Phylogenetic and conserved sequence analysis of PaMYB protein sequences revealed that group member sequences are conserved and clustered together. No 3R-MYBs or 4R-MYBs were identified; this is not surprising as only four 3R-MYBs and no 4R-MYBs were identified in *C. camphora* (Luan et al., 2022). In total, 23 MYBs could

not be classified. InterPro analysis confirmed that these proteins contained DNA-binding domains and could still be functional MYB-like TFs. Phylogenetic comparisons with AtMYBs showed that MYBs with different functions group into different clades (Hernández-Hernández et al., 2020). Further functional studies are needed to investigate whether PaMYBs that group closely with AtMYBs share functionality. Gene structure analysis showed that *PaMYB* genes contained similar intron numbers compared to other plant species. In *Arabidopsis* and rice (*Oryza sativa*), 4.5% and 10%, respectively, of *MYB* genes were intronless, while 38% and 26% contained two introns, respectively (Katiyar et al., 2012). In avocado, 3% of the *MYB* genes were intronless, and 39% contained two introns. This shows that the number of *MYB* introns are conserved between species, providing evidence for functional constraints (Chang et al., 2020).

FIGURE 6 The level of expression of *AP2/ERFs* transcription factors in partially resistant Dusa and susceptible R0.12 avocado rootstocks following *Phytophthora cinnamomi* inoculation. (a) Heatmap showing expression differences of 116 *AP2/ERFs* (as $\log_2$fold-change values; $\log_2$FC) compared to mock-inoculated samples. (b) Heatmap of 87 *AP2/ERFs* genes showing significant differences in expression level following *P. cinnamomi* inoculation when compared between the two rootstocks, with R0.12 set as the reference. $\log_2$FC values larger than zero (red) indicate higher expression levels in Dusa, and $\log_2$FC values smaller than zero (blue) indicate higher expression in R0.12. (+ symbols indicate significance, $\log_2$FC ≥ |1|, $p ≤ 0.05$; MI, mock-inoculated).

The remaining *PaMYB* genes contained higher intron numbers (>6) compared to *Arabidopsis* and rice. Similarly, high intron numbers were observed in *Populus trichocarpa* and *Salix purpurea MYB* genes, showing that complicated exon–intron structures may be functionally significant (Carmel et al., 2007; Gorlova et al., 2014; Zhou et al., 2021). One notable *PaMYB* gene contained the highest number of 34 introns, compared to other plant species. Whether these high intron numbers are the result of 'intron-gain' events form part of the debate regarding intron origins (Feng et al., 2017; Koonin, 2006; Rogozin et al., 2012).

All WRKY group and subgroup members, except for one IIe, grouped together following phylogenetic analysis. These results indicate that the protein sequences are highly conserved and could indicate the importance of proper WRKY function; this is expected because WRKY TFs play important roles in many cellular possesses (Chen et al., 2019). Phylogenetic analysis between AtWRKYs and PaWRKYs showed that a larger number of PaWRKYs grouped with defence-related AtWRKYs. Future research could investigate expression levels of *PaWRKYs*, closely related to non-defence-related AtWRKYs, during growth and development to validate phylogenetic results. The analysis of exon–intron boundaries revealed that gene structures were not conserved between WRKY members belonging to the same group/subgroup. These results were also observed in *Arabidopsis, Solanum commersonii, Solanum chacoense* and *Liriodendron chinense* (Sultan et al., 2016; Villano et al., 2020; Wu et al., 2022). In contrast, conserved *WRKY* gene structure was seen in *Camellia sinensis*; structural diversity of *WRKY* genes between plant species could indicate diversification and neofunctionalization (Panchy et al., 2016;

Shiu & Bleecker, 2003; Song et al., 2023; Wang et al., 2019). This hypothesis regarding structural diversity is supported by the fact that we did not identify any *WRKY* genes without introns, which was also seen for all species mentioned above. Furthermore, *PaWRKYs* contained a higher number of introns compared to *L. chinense WRKYs*, which is a close relative to avocado (Renner, 1999). An average of two introns were seen in *L. chinense*, with five being the maximum number within a gene. Five introns were seen for many *PaWRKYs*, with one *PaWRKY* (Peame105C01g048210.1) containing 11 introns. The fact that *PaWRKYs* contain higher intron numbers, yet still show conserved protein structures, is indicative of functional constraints on evolutionary processes (Chen et al., 2019; Gorlova et al., 2014; Jo & Choi, 2015; Liu et al., 2021; Rigau et al., 2019).

Phylogenetic analysis of PaAP2/ERF sequences revealed both sequence and domain structure conservation—as with MYBs and WRKYs, this indicates the importance of functional maintenance for these TFs. Furthermore, the structural similarity within PaAP2/ERF groups, and similarity to AtAP2/ERF sequences, indicates that these PaAP2/ERFs may share similar functions (Choi et al., 2023). Exon–intron analysis showed that the structures of AP2-encoding genes are more complex compared to DREB, RAV and ERF-encoding genes. This trend has also been observed in other plant species, including rice, *Saccharum spontaneum*, *Eschscholzia californica* and *Elaeis guineensis* (Li et al., 2020; Rashid et al., 2012; Yamada et al., 2020; Zhou & Rajesh, 2021). It is hypothesized that the small size of this group is attributed to *AP2* gene duplication events occurring after the origin of introns, with these introns impeding further duplication events (Yamada et al., 2020). It has also been hypothesized that the intronless nature of DREB, ERF and RAV-encoding genes accelerates transcription, and thus, response of these genes to environmental stress (Yamada et al., 2020). Avocado DREB-, RAV- and ERF-encoding genes mainly consisted of a single exon, whereas AP2-encoding genes contained nine exons on average—a higher average in relation to the plant species mentioned above. The number of intronless *PaAP2/ERF* (67%) genes was also less compared to other species, where 72.4% of *AP2/ERFs* did not contain introns. Thus, *PaAP2/ERF* genes follow the same trend of having higher intron numbers compared to other plant species, as seen with *PaMYB* and *PaWRKY* genes.

The expression patterns for *PaMYB* and *PaWRKY* TFs clearly indicate separate groups of co-expressed genes. For example, with both TF families, a group of genes were either upregulated or downregulated during early time points post-inoculation, followed by either downregulation or upregulation, respectively. This may indicate that the different groups of co-expressed genes have different regulatory roles, ultimately contributing to the activation and maintenance of immune responses. These results were also observed in *Arabidopsis*, *Dendrobiam catenatum* and *Nicotiana tabacum* plants exposed to different stresses (Bi et al., 2020; Yang et al., 2022; Zhang et al., 2021). *PaMYB* and *PaWRKY* genes, which grouped closely with AtMYBs and AtWRKYs with growth-related function, were mostly upregulated at 6, 12 and 24 hpi. Previous research suggested that *P. cinnamomi* is in a biotrophic phase at these time points, and we hypothesized that a higher number of *PaMYBs* and *PaWRKYs* related to defence-AtWRKYs would thus be upregulated (Backer et al., 2022; Engelbrecht & van den Berg, 2013; van den Berg et al., 2018). Both growth-related MYB and WRKY TFs have been shown to affect callose deposition—important for both cellular growth and defence (Bonke et al., 2003; Pillai et al., 2018). During *P. cinnamomi* infection of avocado, callose deposition would hinder cellular penetration of hyphae; furthermore, in another partially resistant rootstock (R0.06), increased callose deposition was observed at 6, 12, 24 and 48 hpi, with fewer *P. cinnamomi* hyphae present (van den Berg et al., 2018). Based on these results, we suspect that *PaMYBs* and *PaWRKYs* with growth-related functions could regulate the expression of genes responsible for callose synthesis. Lignin deposition was, however, observed in the susceptible R0.12 at 6, 12, 24 and 48 hpi by van den Berg et al. (2018), but absent in the partially resistant R0.06 rootstock. Some *PaMYBs* and *PaWRKYs* were upregulated at 6 hpi in R0.12, which did not have expression level differences in Dusa. We could thus speculate that these TFs may regulate lignin synthesis (Teng et al., 2021; Xiao et al., 2021). Lastly, passive defence responses including rapid root growth and feeder root regeneration have been shown to enhance the resistance of avocado rootstocks towards *P. cinnamomi* and to reduce infection symptoms (Sánchez-Pérez et al., 2009). The increased expression levels observed for growth-related *PaMYBs* and *PaWRKYs* in Dusa may contribute to the activation of root growth and regeneration, reducing the impact of *P. cinnamomi* infection (Chen et al., 2022; Grunewald et al., 2012).

The decreased expression of *PaWRKYs* closely related to defence-AtWRKYs may indicate that these TFs have a suppressive effect on the regulated DRGs. Thus, decreased *PaWRKY* expression would lead to higher DRG expression and enhanced defence activation. This was observed for AtWRKY70, where *Atwrky70* mutant plants showed pathogen-independent defence activation (Zhou et al., 2018). The expression level for these *PaWRKY* genes was higher in R0.12 at early infection time points compared to Dusa and may indicate stronger DRG suppression in this rootstock. This may ultimately lead to defence responses not being activated as strongly and increased susceptibility. The increased expression of *PaMYB* and *PaWRKY* genes, which group closely with defence-related AtMYBs and WRKYs, at 120 hpi were unexpected as these defence-related TFs often activate the expression of many *PRR* and *NLR* genes. Previous studies reported increased expression levels of most *PaPRRs* and *PaNLRs* at 6, 12 and 24 hpi in Dusa and R0.12 (Backer et al., 2022; Fick, Swart, Backer, et al., 2022). Thus, it was expected that a higher number of defence-associated *PaMYBs* and *PaWRKYs* would be expressed at these early time points. However, systemic acquired resistance (SAR) could induce the expression of defence-related *TF* genes further from the point of infection (Gao et al., 2015). Because entire root samples were used for RNA-seq analysis, gene transcription in cells further from the point of infection could influence the results. SAR would prime defence responses away from infection sites to prepare cells for future infection. This would explain why the expression levels of *PRR* genes, which encode receptor-like kinases, increase at 120

hpi in both rootstocks, as reported by Backer et al. (2022). A higher abundance of these receptors in uninfected cells would lead to stronger immune response activation once infection does occur (Andam et al., 2020; Palaniyandi & Muthuswamy, 2017). Thus, increased expression of defence-associated *TF* genes would be seen during later infection time points.

PaAP2/ERF genes did not clearly show different groups of co-expressed genes. Only two genes (Peame105C06g007640 and Peame105C02g034190) were strongly upregulated at 6, 12 and 24 hpi in Dusa, while all other *PaAP2/ERF* genes were downregulated. These downregulated genes included 11 of the 24 sequences identified to have repressive EAR motifs. This suggests that the repressive effect these TFs have on DRG expression is abolished (Xie et al., 2019). In the susceptible R0.12, the expression of most *AP2/ERF* genes increased as pathogen infection progressed, with expression levels being significantly higher in R0.12 compared to Dusa at 12 and 24 hpi. Along with this, the expression of EAR motif-containing sequences increased, suggesting increased suppression on the genes these TFs regulate. These results correlate with lower levels of *PRR* and *NLR* gene expression at 12 and 24 hpi in R0.12 reported by Backer et al. (2022) and Fick, Swart, Backer, et al. (2022). *PaAP2/ERF* with homologues associated with fatty acid accumulation in Hass avocado was also downregulated at early infection time points in both rootstocks. These genes were only downregulated at 6 hpi in susceptible R0.12. Interestingly, no AP2-encoding genes were upregulated in Dusa, while three of these genes were upregulated at different time points in R0.12. AP2 proteins mainly regulate cellular growth and differentiation and could indicate the misregulation of these genes in R0.12 during *P. cinnamomi* infection (Bolton, 2009; Gorshkov & Tsers, 2022; Pande et al., 2018). Increased fatty acid accumulation and cellular growth could lead to fewer resources being available for defence, which could lead to decreased resistance (Bolton, 2009; Gorshkov & Tsers, 2022; He & Ding, 2020).

The expression patterns for these three major TF families may indicate that the susceptible R0.12 is slowly shutting down biotrophic-related immune responses at 12 and 24 hpi, while these responses remain activated in the partially resistant Dusa at 24 hpi. Furthermore, these expression patterns may explain the differences in callose deposition, *PRR* and *NLR* expression patterns previously observed within resistant and susceptible rootstocks following *P. cinnamomi* infection (Backer et al., 2022; Fick, Swart, Backer, et al., 2022; van den Berg et al., 2018). Because plant–pathogen interactions are extremely complex, the cause of these observations can only be hypothesized. One hypothesis is that *P. cinnamomi* switches to a necrotrophic phase earlier in the susceptible rootstock R0.12 compared to Dusa, due to the pathogen having an increased growth rate in R0.12 (Engelbrecht et al., 2013). Another hypothesis proposes that *P. cinnamomi* is able to suppress immune responses in R0.12 more strongly compared to Dusa. Some oomycete effectors, such as the *Phytophthora sojae* RxLR Avr3b and PsAvh238, suppress plant immune responses (Kong et al., 2015; Saraiva et al., 2023; Yang

et al., 2019). *P. cinnamomi* RxLRs with high sequence similarity to these *P. sojae* RxLRs have been identified by Joubert et al. (2021), and it would be interesting to investigate whether the effect of these RxLRs differ between the two rootstocks. Studying avocado–*P. cinnamomi* molecular interactions will provide a better understanding of how successful immune responses are activated, and thus how to select rootstocks with enhanced resistance towards this devastating pathogen.

This is the first study to identify and characterize avocado MYB- and WRKY-encoding genes, and to investigate the expression of *MYB*, *WRKY* and *AP2-ERF* genes in two avocado rootstocks following *P. cinnamomi* inoculation. Gene structure analysis of these three TF families revealed more complex gene structures, with higher gene intron numbers, in contrast to *TF* genes in other plant species, hinting at the interesting evolutionary processes shaping these gene families. The conservation of protein sequences and motifs, however, emphasizes the functional importance of these TFs. Significant differences in expression patterns were seen for these TF families between the partially resistant Dusa and susceptible R0.12 rootstocks, following *P. cinnamomi* inoculation. The misregulation of some TFs was also observed in R0.12 and suggests that unfavourable growth-related pathways are being activated, rather than defence responses. Thus, this study highlights the importance of studying the regulatory aspects of DRG expression and provides possible evidence of immune response manipulation by *P. cinnamomi*. Growth and defence pathways are extremely complex, and more research is needed to validate the function of these TFs.

4 | EXPERIMENTAL PROCEDURES

4.1 | *MYB, WRKY* and *AP2/ERF* identification

For MYB, WRKY and AP2/ERF identification, the full repertoire of *P. americana* 'West-Indian' pure accession protein sequences based on whole-genome annotation (Avocado Genome Consortium, unpublished data) were analysed using blastp in the BLAST+ suite, with an expected value (E) cut-off of $1e^{-5}$ and only the top match for each query being considered (Camacho et al., 2009). To identify any TF sequences incorrectly annotated during blastp analysis, the identified protein sequences were used to build HMMER profiles for each TF type using HMMER v. 3.3.2, following sequence alignment using the online Clustal Omega tool (https://www.ebi.ac.uk/Tools/msa/clustalo/). HMMER searches were then performed using whole-genome protein sequences (Eddy, 1996). Putative MYB, WRKY and AP2/ERF protein sequences were validated by protein domain analysis using the PlantRegMap Plant Transcription Factor Database (PlantTFDB v. 5.0; http://plantregmap.gao-lab.org) (Jin et al., 2017; Tian et al., 2020) and the InterPro website database (https://www.ebi.ac.uk/interpro/; accessed March 2023) (Paysan-Lafosse et al., 2023). PROSITE profiles, PROSITE patterns, and Pfam member databases were selected during InterPro

analyses. Lastly, the West-Indian genome GFF3 file was used to create gene structure figures for each *TF* gene using the TBtools software (Chen et al., 2020).

4.2 | Conserved motif and phylogenetic analysis

Conserved motifs for the three TF families were predicted by protein sequence analyses with the MEME Suite web server v. 5.5.1 (https://meme-suite.org/meme/, accessed March 2023). Parameters were set to a maximum number of motifs of 15, with an optimum motif width of ≥6 and ≤50 amino acids. Only conserved motifs with a significant *p*-value ($p \leq 0.05$) were considered. The conserved motifs were used to classify MYB TFs as 1R-MYB-encoding, R2R3-MYB-encoding, 3R-MYB-encoding or 4R-MYB-encoding TFs (Pu et al., 2020; Xie et al., 2021). WRKY TF groups were identified based on the number of WRKY motifs within each sequence, and the motif sequence upstream from the WRKY motif (Sun et al., 2022; Zhang & Wang, 2005). AP2/ERFs were grouped into different subfamilies based on either having an AP2, DREB, ERF or RAV motif (Yamada et al., 2020). Phylogenetic tree topology was determined for each avocado TF family following ClustalW alignment using MEGA 11.0 software, with the neighbourhood-joining method, Jones–Thornton–Taylor (JTT) method and 1000 bootstrap replications. The resulting phylogenetic trees, together with MEME motif data, were imported into iTOL v. 6.7.2 for visualization (Letunic & Bork, 2021).

Phylogenetic analysis was conducted using avocado TF protein sequences and previously identified *Arabidopsis* TF sequences experimentally shown to either regulate growth- or defence-related pathways. This was done to assign possible regulatory roles to the identified avocado TFs. Fifty-four AtMYB sequences were obtained from Hernández-Hernández et al. (2020), 34 AtWRKY sequences from Bakshi and Oelmüller (2014) and Rushton et al. (2010) and 21 AtAP2/ERF sequences from Licausi et al. (2013) and Xie et al. (2019). AP2/ERF sequences (137) identified in the avocado Hass cultivar were also included during the phylogenetic analysis for this TF family (Ge et al., 2021). The identified sequences (File S1) were downloaded from the National Centre for Biotechnology Information (NCBI) database (https://www.ncbi.nlm.nih.gov). For each TF family, avocado and *Arabidopsis* sequences were aligned using ClustalW alignment in MEGA 11.0, followed by maximum-likelihood phylogenetic analysis using IQ-tree v. 1.6.12 (Trifinopoulos et al., 2016) with 1000 bootstrap replications. The ModelFinder option identified JTT + G4 as the optimal substitution model for the MYB dataset, and JTT + F + G4 for the WRKY and AP2/ERF datasets.

4.3 | Plant material

The inoculation trial was previously conducted and published by Backer et al. (2022). Briefly, 2-year-old Dusa (partially resistant to

P. cinnamomi) and R0.12 (susceptible) avocado clonal plants were obtained from Westfalia Innovation and Technology (Tzaneen, Limpopo, South Africa). Plants were inoculated by submerging the roots and lower stem for 2h in a *P. cinnamomi* (isolate GBK4) zoospore suspension (1.4×10^5 zoospores/mL), which was prepared as described in Engelbrecht and van den Berg (2013). Plants submerged in distilled water served as controls (mock-inoculated). Root samples were harvested at 6, 12, 24 and 120 hpi. Three replicate samples, with three plants per replicate, were used for each time point. Samples from the control plant group were only taken at 24 hpi due to limited plants.

4.4 | RNA extraction and sequencing

RNA was extracted from all samples using a modified CTAB RNA extraction protocol (Engelbrecht & van den Berg, 2013). RNase-free DNase (Fermentas Life Sciences) was used to treat the samples for potential DNA contamination, using the manufacturer's guidelines. The samples were then purified using the RNeasy Mini-Elute cleanup kit (Qiagen) following the manufacturer's guidelines. Lastly, 1 μg purified RNA from biological replicates were combined to serve as samples that were used for each respective library. RNA-sequencing (RNA-seq) was performed by Macrogen Inc. (Seoul, South Korea) on an Illumina HiSeq platform, using the PE150 mode. A minimum raw read count of 80 million was obtained per sample.

4.5 | RNA-sequencing data processing

Illumina adapters and low-quality bases were removed from the raw RNA-seq data using Trimmomatic v. 0.39. FastQC v. 0.11.9 (Andrews, 2010; Bolger et al., 2014) was used to assess the read quality, which was then summarized using MultiQC v. 1.9 (Ewels et al., 2016). The *P. americana* 'West-Indian' pure accession genome was concatenated and used for the alignment of RNA-seq data, using HISAT2 v. 2.0.6 (Kim et al., 2019). Samtools (Li et al., 2009) and Portcullis v. 1.2.0 (Mapleson et al., 2018) was used to process and combine the alignment files and to obtain high-confidence splice junctions. HISAT2 was used to perform a second alignment using the high-confidence splice junctions that were obtained from Portcullis. Samtools idxstats and flagstat were used to calculate alignment statistics. Lastly, transcripts per million (TPMs) were calculated using StringTie v. 2.1.4 (Pertea et al., 2015).

4.6 | Analyses of differential gene expression

Read counts, informed by the *P. americana* genome, were quantified at gene levels using featureCounts v. 2.0.1 (Liao et al., 2014). DeSeq2 v. 1.32.0 (Love et al., 2014) was used to analyse the resulting data in R v. 4.0.4 (R Core Team, 2021). Data were removed from the dataset

if transcript counts were below 10 reads per library, or if no read data were available. Control (mock-inoculated) libraries for Dusa or R0.12 were set as reference libraries, to which Dusa and R0.12 inoculated libraries were compared, respectively. For expression-level comparisons between the two rootstocks, R0.12 libraries were set as reference libraries. Differentially expressed genes (DEGs) were identified by Wald tests, and multiple hypothesis testing correction was done by Benjamini–Hochberg false discovery rate methods. Genes with significant differences in expression levels were defined as genes with a $\log_2$fold-change ($\log_2$FC) value of more than +1, or smaller than −1, as well as having a significant p-value ($p < 0.05$). Heatmaps for data visualization were produced using the pheatmap v. 1.0.12 package in RStudio v. 1.4.1106 (RStudio Team, 2020).

DATA AVAILABILITY STATEMENT

The data sets used in this study can be found in online repositories. Raw RNA-seq data used in this study has been deposited in the Sequence Read Archive of NCBI GenBank at https://www.ncbi.nlm.nih.gov/sra under accession number PRJNA675400.

ORCID

Alicia Fick https://orcid.org/0009-0002-7455-0411

Velushka Swart https://orcid.org/0000-0001-9687-5650

REFERENCES

Ali, M.A., Abbas, A., Kreil, D.P. & Bohlmann, H. (2013) Overexpression of the transcription factor RAP2.6 leads to enhanced callose deposition in syncytia and enhanced resistance against the beet cyst nematode *Heterodera schachtii* in *Arabidopsis* roots. *BMC Plant Biology*, 13, 47.

Ambawat, S., Sharma, P., Yadav, N. & Yadav, R. (2013) MYB transcription factor genes as regulators for plant responses: an overview. *Physiology and Molecular Biology of Plants*, 19, 307–321.

Andam, A., Azizi, A., Majdi, M. & Abdolahzadeh, J. (2020) Comparative expression profile of some putative resistance genes of chickpea genotypes in response to ascomycete fungus, *Ascochyta rabiei* (Pass.) Labr. *Brazilian Journal of Botany*, 43, 123–130.

Andrews, S. (2010) FastQC: a quality control tool for high throughput sequence data. Babraham Bioinformatics: Babraham Institute. Available from: https://www.bioinformatics.babraham.ac.uk/projects/fastqc/ [Accessed 11th February 2021]

Backer, R., Engelbrecht, J. & van den Berg, N. (2022) Differing responses to *Phytophthora cinnamomi* infection in susceptible and partially resistant *Persea americana* (Mill.) rootstocks: a case for the role of receptor-like kinases and apoplastic proteases. *Frontiers in Plant Science*, 13, 928176.

Backer, R., Mahomed, W., Reeksting, B.J., Engelbrecht, J., Ibarra-Laclette, E. & van den Berg, N. (2015) Phylogenetic and expression analysis of the *NPR1*-like gene family from *Persea americana* (Mill.). *Frontiers in Plant Science*, 6, 300.

Bahari, M.N.A., Sakeh, N.M., Abdullah, S.N.A., Ramli, R.R. & Kadkhodaei, S. (2018) Transciptome profiling at early infection of *Elaeis guineensis* by *Ganoderma boninense* provides novel insights on fungal transition from biotrophic to necrotrophic phase. *BMC Plant Biology*, 18, 377.

Bakshi, M. & Oelmüller, R. (2014) WRKY transcription factors: jack of many trades in plants. *Plant Signaling and Behaviour*, 9, e27700.

Berrocal-Lobo, M., Molina, A. & Solano, R. (2002) Constitutive expression of Ethylene-Response-Factor1 in *Arabidopsis* confers resistance to several necrotrophic fungi. *The Plant Journal*, 29, 23–32.

Bi, H., Zhao, Y., Li, H. & Liu, W. (2020) Wheat heat shock factor TaHsfA6f increases ABA levels and enhances tolerance to multiple abiotic stresses in transgenic plants. *International Journal of Molecular Sciences*, 21, 3121.

Bolger, A.M., Lohse, M. & Usadel, B. (2014) Trimmomatic: a flexible trimmer for Illumina sequence data. *Bioinformatics*, 30, 2114–2120.

Bolton, M.D. (2009) Primary metabolism and plant defense—fuel for the fire. *Molecular Plant–Microbe Interactions*, 22, 487–497.

Bonke, M., Thitamadee, S., Mähönen, A.P., Hauser, M.T. & Helariutta, Y. (2003) APL regulates vascular tissue identity in *Arabidopsis*. *Nature*, 426, 181–186.

Camacho, C., Coulouris, G., Avagyan, V., Ma, N., Papadopoulos, J., Bealer, K. et al. (2009) BLAST+: architecture and applications. *BMC Bioinformatics*, 10, 421.

Cao, Y., Li, K., Li, Y., Zhao, X. & Wang, L. (2020) MYB transcription factors as regulators of secondary metabolism in plants. *Biology*, 9, 61.

Carmel, L., Rogozin, I.B., Wolf, Y.I. & Koonin, E.V. (2007) Evolutionarily conserved genes preferentially accumulate introns. *Genome Research*, 17, 1045–1050.

Chang, X., Xie, S., Wei, L., Lu, Z., Chen, Z.H., Chen, F. et al. (2020) Origins and stepwise expansion of R2R3-MYB transcription factors for the terrestrial adaptation of plants. *Frontiers in Plant Science*, 11, 575360.

Chaw, S.M., Liu, Y.C., Wu, Y.W., Wang, H.Y., Lin, C.Y.I., Wu, C.S. et al. (2019) Stout camphor tree genome fills gaps in understanding of flowering plant genome evolution. *Nature Plants*, 5, 63–73.

Chen, C., Chen, H., Zhang, Y., Thomas, H.R., Frank, M.H., He, Y. et al. (2020) TBtools: an integrative toolkit developed for interactive analyses of big biological data. *Molecular Plant*, 13, 1194–1202.

Chen, X., Li, C., Wang, H. & Guo, Z. (2019) WRKY transcription factors: evolution, binding, and action. *Phytopathology Research*, 1, 13.

Chen, Z., Wu, Z., Dong, W., Liu, S., Tian, L., Li, J. et al. (2022) MYB transcription factors becoming mainstream in plant roots. *International Journal of Molecular Sciences*, 23, 9262.

Choi, J.W., Choi, H.H., Park, Y.S., Jang, M.J. & Kim, S. (2023) Comparative and expression analyses of *AP2/ERF* genes reveal copy number expansion and potential functions of *ERF* genes in *Solanaceae*. *BMC Plant Biology*, 23, 48.

Cui, H., Tsuda, K. & Parker, J.E. (2015) Effector-triggered immunity: from pathogen perception to robust defence. *Annual Review of Plant Biology*, 66, 487–511.

Daniel, X., Lacomme, C., Morel, J.B. & Roby, D. (1999) A novel myb oncogene homologue in *Arabidopsis thaliana* related to hypersensitive cell death. *The Plant Journal*, 20, 57–66.

Deslandes, L., Olivier, J., Theulières, F., Hirsch, J., Feng, D.X., Bittner-Eddy, P., et al. (2002) Resistance to Ralstonia solanacearum in Arabidopsis thaliana is conferred by the recessive RRS1-R gene, a member of a novel family of resistance genes. *Proceedings of the National Academy of Sciences of the United States of America*, 99, 2404–2409.

Ding, L., Xu, X., Kong, W., Xia, X., Zhang, S., Liu, L.W. et al. (2020) Genome-wide identification and expression analysis of rice *NLR* genes responsive to the infections of *Xanthomonas oryzae* pv. *oryzae* and *Magnaporthe oryzae*. *Physiological and Molecular Plant Pathology*, 111, 101488.

Duan, H., Moresco, P. & Champouret, N. (2023) Characterization of host-effector transcription dynamics during pathogen infection in engineered late blight resistant potato. *Transgenic Research*, 32, 95–107.

Dubos, C., Stracke, R., Grotewold, E., Weisshaar, B., Martin, C. & Lepiniec, L. (2010) MYB transcription factors in *Arabidopsis*. *Trends in Plant Science*, 15, 573–581.

Eddy, S.R. (1996) Hidden Markov models. *Current Opinion in Structural Biology*, 6, 361–365.

Ellinger, D. & Voigt, C.A. (2014) Callose biosynthesis in *Arabidopsis* with a focus on pathogen response: what we have learned within the last decade. *Annals of Botany*, 114, 1349–1358.

Engelbrecht, J., Duong, T.A. & van den Berg, N. (2013) Development of a nested quantitative real-time PCR for detecting *Phytophthora cinnamomi* in *Persea americana* rootstocks. *Plant Disease*, 97, 1012–1017.

Engelbrecht, J. & van den Berg, N. (2013) Expression of defence-related genes against *Phytophthora cinnamomi* in five avocado rootstocks. *South African Journal of Science*, 109, 8.

Eulgem, T., Rushton, P.J., Robatzek, S. & Somssich, I.E. (2000) The WRKY superfamily of plant transcription factors. *Trends in Plant Science*, 5, 199–206.

Ewels, P., Magnusson, M., Lundin, S. & Käller, M. (2016) MultiQC: summarize analysis results for multiple tools and samples in a single report. *Bioinformatics*, 32, 3047–3048.

Falak, N., Imran, Q.M., Hussain, A. & Yun, B.W. (2021) Transcription factors as the "Blitzkrieg" of plant defence: a pragmatic view of nitric oxide's role in gene regulation. *International Journal of Molecular Sciences*, 22, 22020522.

Feng, G., Burleigh, J.G., Braun, E.L., Mei, W. & Barbazuk, W.B. (2017) Evolution of the 3R-MYB gene family in plants. *Genome Biology and Evolution*, 9, 1013–1029.

Feng, K., Hou, X.L., Xing, G.M., Liu, J.X., Duan, A.Q., Xu, Z.S. et al. (2020) Advances in AP2/ERF super-family transcription factors in plant. *Critical Reviews in Biotechnology*, 40, 750–776.

Fick, A., Swart, V., Backer, R., Bombarely, A., Engelbrecht, J. & van den Berg, N. (2022) Partially resistant avocado rootstock Dusa® shows prolonged upregulation of *Nucleotide binding-leucine rich repeat* genes in response to *Phytophthora cinnamomi* infection. *Frontiers in Plant Science*, 13, 793644.

Fick, A., Swart, V. & van den Berg, N. (2022) The ups and downs of plant *NLR* expression during pathogen infection. *Frontiers in Plant Science*, 13, 921148.

Gao, Q.M., Zhu, S., Kachroo, P. & Kachroo, A. (2015) Signal regulators of systemic acquired resistance. *Frontiers in Plant Science*, 6, 228.

Ge, Y., Zang, X., Yang, Y., Wang, T. & Ma, W. (2021) In-depth analysis of potential PaAP2/ERF transcription factor related to fatty acid accumulation in avocado (*Persea americana* Mill.) and functional characterization of two *PaAP2/ERF* genes in transgenic tomato. *Plant Physiology and Biochemistry*, 158, 308–320.

Gorlova, O., Fedorov, A., Logothetis, C., Amos, C. & Gorlov, I. (2014) Genes with a large intronic burden show greater evolutionary conservation on the protein level. *BMC Evolutionary Biology*, 14, 50.

Gorshkov, V. & Tsers, I. (2022) Plant susceptible responses: the underestimated side of plant–pathogen interactions. *Biological Reviews*, 97, 45–66.

Grunewald, W., De Smet, I., Lewis, D.R., Löfke, C., Jansen, L., Goeminne, G. et al. (2012) Transcription factor WRKY23 assists auxin distribution patterns during *Arabidopsis* root development through local control on flavonol biosynthesis. *Proceedings of the National Academy of Sciences of the United States of America*, 109, 1554–1559.

Hardham, A.R. & Blackman, L.M. (2018) *Phytophthora cinnamomi*. *Molecular Plant Pathology*, 19, 260–285.

He, M. & Ding, N.Z. (2020) Plant unsaturated fatty acids: multiple roles in stress response. *Frontiers in Plant Science*, 11, 562785.

Hernández-Hernández, B., Tapia-López, R., Ambrose, B.A. & Vasco, A. (2020) R2R3-MYB gene evolution in plants, incorporating ferns into the story. *International Journal of Plant Sciences*, 182, 1–8.

Huang, S., Zhang, X. & Fernando, W.G.D. (2020) Directing trophic divergence in plant–pathogen interactions: antagonistic phytohormones with no doubt? *Frontiers in Plant Science*, 11, 600063.

Jin, J., Tian, F., Yang, D.C., Meng, Y.Q., Kong, L., Luo, J. et al. (2017) PlantTFDB 4.0: toward a central hub for transcription factors and regulatory interactions in plants. *Nucleic Acids Research*, 45(D1), D1040–D1045.

Jo, B.S. & Choi, S.S. (2015) Introns: the functional benefits of introns in genomes. *Genomics & Informatics*, 13, 112–118.

Jones, J.D.G. & Dangl, J.L. (2006) The plant immune system. *Nature*, 444, 323–329.

Joubert, M., Backer, R., Engelbrecht, J. & van den Berg, N. (2021) Expression of several *Phytophthora cinnamomi* putative *RxLRs* provides evidence for virulence roles in avocado. *PLoS One*, 16, e0254645.

Katiyar, A., Smita, S., Lenka, S.K., Rajwanshi, R., Chinnusamy, V. & Bansal, K.C. (2012) Genome-wide classification and expression analysis of MYB transcription factor families in rice and *Arabidopsis*. *BMC Genomics*, 13, 544.

Kim, D., Paggi, J.M., Park, C., Bennett, C. & Salzberg, S.L. (2019) Graph-based genome alignment and genotyping with HISAT2 and HISAT-genotype. *Nature Biotechnology*, 37, 907–915.

Kong, G., Zhao, Y., Jing, M., Huang, J., Yang, J., Xia, Y. et al. (2015) The activation of *Phytophthora* effector Avr3b by plant cyclophilin is required for the nudix hydrolase activity of avr3b. *PLoS Pathogens*, 11, e1005139.

Koonin, E.V. (2006) The origin of introns and their role in eukaryogenesis: a compromise solution to the introns-early versus introns-late debate? *Biology Direct*, 1, 22.

Lai, Z. & Mengiste, T. (2013) Genetic and cellular mechanisms regulating plant responses to necrotrophic pathogens. *Current Opinion in Plant Biology*, 16, 505–512.

Letunic, I. & Bork, P. (2021) Interactive Tree Of Life (iTOL) v5: an online tool for phylogenetic tree display and annotation. *Nucleic Acids Research*, 49, 845–854.

Li, H., Handsaker, B., Wysoker, A., Fennell, T., Ruan, J., Homer, N. et al. (2009) The sequence alignment/map format and SAMtools. *Bioinformatics*, 25, 2078–2079.

Li, P., Chai, Z., Lin, P., Huang, C., Huang, G., Xu, L. et al. (2020) Genome-wide identification and expression analysis of AP2/ERF transcription factors in sugarcane (*Saccharum spontaneum* L.). *BMC Genomics*, 21, 685.

Liao, C.J., Hailemariam, S., Sharon, A. & Mengiste, T. (2022) Pathogenic strategies and immune mechanisms to necrotrophs: differences and similarities to biotrophs and hemibiotrophs. *Current Opinion in Plant Biology*, 69, 102291.

Liao, Y., Smyth, G.K. & Shi, W. (2014) featureCounts: an efficient general purpose program for assigning sequence reads to genomic features. *Bioinformatics*, 30, 923–930.

Licausi, F., Ohme-Takagi, M. & Perata, P. (2013) APETALA2/ethylene responsive factor (AP2/ERF) transcription factors: mediators of stress responses and developmental programs. *New Phytologist*, 199, 639–649.

Liu, H., Lyu, H.M., Zhu, K., van de Peer, Y. & Cheng, Z.M. (2021) The emergence and evolution of intron-poor and intronless genes in intron-rich plant gene families. *The Plant Journal*, 105, 1072–1082.

Lorenzo, O., Piqueras, R., Sánchez-Serrano, J.J. & Solano, R. (2003) Ethylene response Factor1 integrates signals from ethylene and jasmonate pathways in plant defence. *The Plant Cell*, 15, 165–178.

Love, M.I., Huber, W. & Anders, S. (2014) Moderated estimation of fold change and dispersion for RNA-seq data with DESeq2. *Genome Biology*, 15, 550.

Luan, X., Xu, W., Zhang, J., Shen, T., Chen, C., Xi, M. et al. (2022) Genome-scale identification, classification, and expression profiling of MYB transcription factor genes in *Cinnamomum camphora*. *International Journal of Molecular Sciences*, 23, 14279.

Ma, N., Sun, P., Li, Z.Y., Zhang, F.J., Wang, X.F., You, C.X. et al. (2024) Plant disease resistance outputs regulated by AP2/ERF transcription factor family. *Stress Biology*, 4, 2.

Mahiwal, S., Pahuja, S. & Pandey, G.K. (2024) Structural-functional relationship of WRKY transcription factors: unfolding the role of WRKY in plants. *International Journal of Biological Macromolecules*, 257, 128769.

Mapleson, D., Venturini, L., Kaithakottil, G. & Swarbreck, D. (2018) Efficient and accurate detection of splice junctions from RNA-seq with Portcullis. *GigaScience*, 7, giy131.

Matzinger, P. (2007) Friendly and dangerous signals: is the tissue in control? *Nature Immunology*, 8, 11–13.

Mengiste, T., Chen, X., Salmeron, J. & Dietrich, R. (2003) The *BOTRYTIS SUSCEPTIBLE1* gene encodes an R2R3MYB transcription factor protein that is required for biotic and abiotic stress responses in *Arabidopsis*. *The Plant Cell*, 15, 2551–2565.

Mohr, T.J., Mammarella, N.D., Hoff, T., Woffenden, B.J., Jelesko, J.G. & McDowell, J.M. (2010) The *Arabidopsis* downy mildew resistance gene *RPP8* is induced by pathogens and Salicylic acid and is regulated by W-box *cis*-elements. *Molecular Plant–Microbe Interactions*, 23, 1303–1315.

Monteiro, F. & Nishimura, M.T. (2018) Structural, functional, and genomic diversity of plant NLR proteins: an evolved resource for rational engineering of plant immunity. *Annual Review of Phytopathology*, 56, 243–267.

Moore, J.W., Loake, G.J. & Spoel, S.H. (2011) Transcription dynamics in plant immunity. *The Plant Cell*, 23, 2809–2820.

Nakano, T., Suzuki, K., Fujimura, T. & Shinshi, H. (2006) Genome-wide analysis of the *ERF* gene family in *Arabidopsis* and rice. *Plant Physiology*, 140, 411–432.

Ng, D.W., Abeysinghe, J.K. & Kamali, M. (2018) Regulating the regulators: the control of transcription factors in plant defence signaling. *International Journal of Molecular Sciences*, 19, 3737.

Palaniyandi, U. & Muthuswamy, A. (2017) Genotype specific host resistance for *Phytophthora* in black pepper (*Piper nigrum* L.). *Physiological and Molecular Plant Pathology*, 100, 237–241.

Panchy, N., Lehti-Shiu, M. & Shiu, S.H. (2016) Evolution of gene duplication in plants. *Plant Physiology*, 171, 2294–2316.

Pande, A., Saxena, S., Thapliyal, M., Guru, S., Kumar, A. & Arora, S. (2018) Role of AP2/EREBP transcription factor family in environmental stress tolerance. *Cell and Cellular Life Sciences Journal*, 3, 000120.

Paysan-Lafosse, T., Blum, M., Chuguransky, S., Grego, T., Pinto, B.L., Salazar, G.A. et al. (2023) InterPro in 2022. *Nucleic Acids Research*, 51(D1), D418–D427.

Pertea, M., Pertea, G.M., Antonescu, C.M., Chang, T.C., Mendell, J.T. & Salzberg, S.L. (2015) StringTie enables improved reconstruction of a transcriptome from RNA-seq reads. *Nature Biotechnology*, 33, 290–295.

Pillai, S.E., Kumar, C., Patel, H.K. & Sonti, R.V. (2018) Overexpression of a cell wall damage induced transcription factor, OsWRKY42, leads to enhanced callose deposition and tolerance to salt stress but does not enhance tolerance to bacterial infection. *BMC Plant Biology*, 18, 177.

Pu, X., Yang, L., Liu, L., Dong, X., Chen, S., Chen, Z. et al. (2020) Genome-wide analysis of the MYB transcription factor superfamily in *Physcomitrella patens*. *International Journal of Molecular Sciences*, 21, 975.

R Core Team. (2021) *R: a language and environment for statistical computing*. Vienna, Austria: R Foundation for Statistical Computing. Available from: https://www.r-project.org/ [Accessed 17th February 2021]

Rashid, M., Guangyuan, H., Guangxiao, Y., Hussain, J. & Xu, Y. (2012) AP2/ERF transcription factor in rice: genome-wide canvas and syntenic relationships between monocots and eudicots. *Evolutionary Bioinformatics*, 8, EBO.S9369.

Renner, S.S. (1999) Circumscription and phylogeny of the Laurales: evidence from molecular and morphological data. *American Journal of Botany*, 86, 1301–1315.

Rigau, M., Juan, D., Valencia, A. & Rico, D. (2019) Intronic CNVs and gene expression variation in human populations. *PLoS Genetics*, 15, e1007902.

Rogozin, I.B., Carmel, L., Csuros, M. & Koonin, E.V. (2012) Origin and evolution of spliceosomal introns. *Biology Direct*, 7, 11.

RStudio Team. (2020) *RStudio: integrated development for R*. Boston, USA: RStudio, PBC. Available at: http://www.rstudio.com/ [Accessed 22nd March 2024]

Rushton, P.J., Somssich, I.E., Ringler, P. & Shen, Q.J. (2010) WRKY transcription factors. *Trends in Plant Science*, 15, 247–258.

Sánchez-Pérez, J.D.L., Jaimes-Lara, M.G., Salgado-Garciglia, R. & López-Meza, J.E. (2009) Root extracts from Mexican avocado (*Persea americana* var. *drymifolia*) inhibit the mycelial growth of the oomycete *Phytophthora cinnamomi*. *European Journal of Plant Pathology*, 124, 595–601.

Saraiva, M., Ściślak, M.E., Ascurra, Y.T., Ferrando, T.M., Zic, N., Henard, C. et al. (2023) The molecular dialog between oomycete effectors and their plant and animal hosts. *Fungal Biology Reviews*, 43, 100289.

Seo, E.,& Choi, D. (2015) Functional studies of transcription factors involved in plant defences in the genomics era. *Briefings in Functional Genomics*, 14, 260–267.

Seo, P.J. & Park, C.M. (2010) MYB96-mediated Abscisic acid signals induce pathogen resistance response by promoting salicylic acid biosynthesis in *Arabidopsis*. *New Phytologist*, 186, 471–483.

Shen, Q.H., Saijo, Y., Mauch, S., Biskup, C., Bieri, S., Keller, B. et al. (2007) Nuclear activity of MLA immune receptors links isolate-specific and basal disease-resistance responses. *Science*, 315, 1098–1103.

Shiu, S.H. & Bleecker, A.B. (2003) Expansion of the receptor-like kinase/pelle gene family and receptor-like proteins in *Arabidopsis*. *Plant Physiology*, 132, 530–543.

Song, H., Cao, Y., Zhao, L., Zhang, J. & Li, S. (2023) WRKY transcription factors: understanding the functional divergence. *Plant Science*, 334, 111770.

Sultan, S., Ali, M., Atif, R.M., Azeem, F., Nadeem, H., Siddique, M.H. et al. (2016) Genome wide analysis of stress responsive WRKY transcription factors in *Arabidopsis thaliana*. *Turkish Journal of Agriculture-Food Science and Technology*, 4, 279.

Sun, S., Chen, H., Yang, Z., Lu, J., Wu, D., Luo, Q. et al. (2022) Identification of WRKY transcription factor family genes in *Pinus massoniana* Lamb. and their expression patterns and functions in response to drought stress. *BMC Plant Biology*, 22, 424.

Teng, R., Wang, Y., Lin, S., Chen, Y., Yang, Y., Yang, N. et al. (2021) CsWRKY13, a novel WRKY transcription factor of *Camellia sinensis*, involved in lignin biosynthesis and accumulation. *Beverage Plant Research*, 1, 12.

Tian, F., Yang, D.C., Meng, Y.Q., Jin, J. & Gao, G. (2020) PlantRegMap: charting functional regulatory maps in plants. *Nucleic Acids Research*, 48(D1), D1104–D1113.

Tiwari, S.B., Belachew, A., Ma, S.F., Young, M., Ade, J., Shen, Y. et al. (2012) The EDLL motif: a potent plant transcriptional activation domain from AP2/ERF transcription factors. *The Plant Journal*, 70, 855–865.

Trifinopoulos, J., Nguyen, L.T., von Haeseler, A. & Minh, B.Q. (2016) W-IQ-TREE: a fast online phylogenetic tool for maximum likelihood analysis. *Nucleic Acids Research*, 44(W1), W232–W235.

van den Berg, N., Christie, J.B., Aveling, T.A.S. & Engelbrecht, J. (2018) Callose and β-1,3-glucanase inhibit *Phytophthora cinnamomi* in a resistant avocado rootstock. *Plant Pathology*, 67, 1150–1160.

van den Berg, N., Swart, V., Backer, R., Fick, A., Wienk, R., Engelbrecht, J. et al. (2021) Advances in understanding defence mechanisms in *Persea americana* against *Phytophthora cinnamomi*. *Frontiers in Plant Science*, 12, 636339.

Villano, C., Esposito, S., D'Amelia, V., Garramone, R., Alioto, D., Zoina, A. et al. (2020) *WRKY* genes family study reveals tissue-specific and stress-responsive TFs in wild potato species. *Scientific Reports*, 10, 7196.

Wang, P., Yue, C., Chen, D., Zheng, Y., Zhang, Q., Yang, J. et al. (2019) Genome-wide identification of *WRKY* family genes and their response to abiotic stresses in tea plant (*Camellia sinensis*). *Genes & Genomics*, 41, 17–33.

Wani, S.H., Anand, S., Singh, B., Bohra, A. & Joshi, R. (2021) WRKY transcription factors and plant defence responses: latest discoveries and future prospects. *Plant Cell Reports*, 40, 1071–1085.

Wu, W., Zhu, S., Xu, L., Zhu, L., Wang, D., Liu, Y. et al. (2022) Genome-wide identification of the *Liriodendron chinense WRKY* gene family and its diverse roles in response to multiple abiotic stress. *BMC Plant Biology*, 22, 25.

Xiao, R., Zhang, C., Guo, X., Li, H. & Lu, H. (2021) MYB transcription factors and its regulation in secondary cell wall formation and lignin biosynthesis during xylem development. *International Journal for Molecular Sciences*, 22, 3560.

Xie, F., Hua, Q., Chen, C., Zhang, Z., Zhang, R., Zhao, J. et al. (2021) Genome-wide characterization of R2R3-MYB transcription factors in pitaya reveals a R2R3-MYB repressor *HuMYB1* involved in fruit ripening through regulation of betalain biosynthesis by repressing betalain biosynthesis-related genes. *Cells*, 10, 1949.

Xie, Z., Nolan, T.M., Jiang, H. & Yin, Y. (2019) AP2/ERF transcription factor regulatory networks in hormone and abiotic stress responses in *Arabidopsis*. *Frontiers in Plant Science*, 10, 228.

Yamada, Y., Nishida, S., Shitan, N. & Sato, F. (2020) Genome-wide identification of AP2/ERF transcription factor-encoding genes in California poppy (*Eschscholzia californica*) and their expression profiles in response to methyl jasmonate. *Scientific Reports*, 10, 18066.

Yang, B., Wang, Y., Guo, B., Jing, M., Zhou, H., Li, Y. et al. (2019) The *Phytophthora sojae* RXLR effector Avh238 destabilizes soybean Type2 GmACSs to suppress ethylene biosynthesis and promote infection. *New Phytologist*, 222, 425–437.

Yang, F., Li, W. & Jørgensen, H.J.L. (2013) Transcriptional reprogramming of wheat and the hemibiotrophic pathogen *Septoria tritici* during two phases of the compatible interaction. *PLoS One*, 8, e81606.

Yang, J., Zhang, B., Gu, G., Yuan, J., Shen, S., Jin, L. et al. (2022) Genome-wide identification and expression analysis of the R2R3-MYB gene family in tobacco (*Nicotiana tabacum* L.). *BMC Genomics*, 23, 432.

Yun, S.H., Noh, B. & Noh, Y.S. (2023) Plant immunity: a plastic system operated through cell-fate transition. *Journal of Plant Biology*, 66, 193–206.

Zhang, C., Jiao, C., Sun, X. & Li, X. (2023) A MYB transcription factor atlas provides insights into the evolution of environmental adaptations in plants. *International Journal of Molecular Sciences*, 24, 2566.

Zhang, C., Ma, R., Xu, J., Yan, J., Guo, L., Song, J. et al. (2018) Genome-wide identification and classification of *MYB* superfamily genes in peach. *PLoS One*, 13, e0199192.

Zhang, T., Cui, Z., Li, Y., Kang, Y., Song, X., Wang, J. et al. (2021) Genome-wide identification and expression analysis of *MYB* transcription factor superfamily in *Dendrobium catenatum*. *Frontiers in Genetics*, 12, 714696.

Zhang, Y. & Wang, L. (2005) The WRKY transcription factor superfamily: its origin in eukaryotes and expansion in plants. *BMC Evolutionary Biology*, 5, 1.

Zheng, Z., Qamar, S.A., Chen, Z. & Mengiste, T. (2006) *Arabidopsis* WRKY33 transcription factor is required for resistance to necrotrophic fungal pathogens. *The Plant Journal*, 48, 592–605.

Zhou, F., Chen, Y., Wu, H. & Yin, T. (2021) Genome-wide comparative analysis of R2R3-MYB gene family in *Populus* and *Salix* and identification of male flower bud development-related genes. *Frontiers in Plant Science*, 12, 721.

Zhou, J., Tang, X. & Martin, G.B. (1997) The Pto kinase conferring resistance to tomato bacterial speck disease interacts with proteins that bind a *cis*-element of pathogenesis-related genes. *The EMBO Journal*, 16, 3207–3218.

Zhou, L. & Rajesh, Y. (2021) Genome-wide identification and characterization of AP2/ERF transcription factor family genes in oil palm under abiotic stress conditions. *International Journal of Molecular Sciences*, 22, 2821.

Zhou, M., Lu, Y., Bethke, G., Harrison, B.T., Hatsugai, N., Katagiri, F. et al. (2018) WRKY70 prevents axenic activation of plant immunity by direct repression of *SARD1*. *New Phytologist*, 217, 700–712.

SUPPORTING INFORMATION

Additional supporting information can be found online in the Supporting Information section at the end of this article.